Sirte University Scientific Journal(Applied Sciences) Vol.9 (2), December.2019

Potentials and Prospects of Numerical Investigation of the Thermal Efficiency Optimization in Radiant Tube Burners

E. M. Elmabrouk[1], Imhamed M. Saleh[2] and Mohamed Abdelslam M. saad[3]

e-mail: e.m.elmabrouk@su.edu.ly

[1,3]Department of Chemical Engineering, Sirte University
[2]Department of Mechanical Engineering, Sirte University

Abstract

The paper is designed to present optimization of the radiant tube burners efficiency vital to maximize the heat transfer and minimize the energy input while operating at acceptable pollutant emission levels. The aim is to help demonstrate its value to the country's citizens in providing visible and tangible results by presenting strategy on how to combat the impact of rising fuel prices and the need to comply stringent pollutant emission standards. A numerical study of the combustion and heat transfer process in single-end radiant (SER) tubular burners is presented. Finally the potential benefits of the discrete transfer radiation by method (DTRM) with the weighted sum grey gas (WSGG) model (none grey model) is applied in the simulations of combustion inside a radiation tube burner to calculate the thermal radiation

Keywords: *Radiant Tube Burners; CFD Simulation; Combustion; radiation tube; Weighted Sum Grey Gas; HiTAC technology*

1. Introduction

Preheating a combustible mixture by recycling heat from exhaust gases is considered as an effective method for fuel saving. Katsuki, M et al (1998) stated that flue gas heat circulation is becoming an attractive technique for the future design of industrial furnaces, particularly if fuel saving is a concern. On the other hand, Masters, J et al (1979) and Hiroshi et al (2003) claimed that preheated air with a temperature of 873 K could reduce the fuel input rate to 30% and so reduce carbon dioxide emissions. In addition, if 1273 K air is obtained the reduction of fuel consumption reaches 50%. Radiation is particularly important in the radiation tubes and influences both the combustion and the heat transfer process. The products of natural gas combustion include species such as CO_2 and H_2O, which are spectrally selective absorbers and emitters of thermal radiationH.C. Hottel(1967), R. Siegel et al (1992) and H. Ramamurthy et al (1995).

Researches carried out by Keramida et al (2000) and Elmabrouk et al (2012) aimed at numerically examining a turbulent, non-premixed, natural gas flame with and without consideration of the effects of radiation . The results have confirmed that the effect of thermal radiation is important on flame temperature predictions.

As discussed by Yu et al (2000), Bidi et al (2008) and Guihua et al (2011), the non-gray gases, water vapour and carbon dioxide, are necessarily produced in industrial energy systems. The weighted sum of gray gases model (WSGGM), is one of the simplified models that can reasonably be used in a practical application. In this study, the radiation models of DTRM and WSGGMare applied for the CFD simulation of the combustion and heat transfer in radiation tube burners.

CFD simulations in this work are carried out to examine the influence of the bluff body on combustion, the effect of flue gas recirculation, the effect of high temperature air combustion and burner thermal efficiency

2. An Appraisal of Temperature Measurements

This work is based on the previous experimental work published by Elmabrouk et al (2012), The dimensions and structure of the SET burners are illustrated in Fig. 1. The SET burner consists of a recuperative section and a radiant heating section. The ceramic tube is positioned in the heating section to form an inner flame tube and the annular outer flow channel. The radiant tube has a free length of 1,293 mm inside the furnace and an outer diameter of 150 mm. The flame tube consists of three segments, which have an overall length of 1,050 mm and an inner diameter of 92 mm.

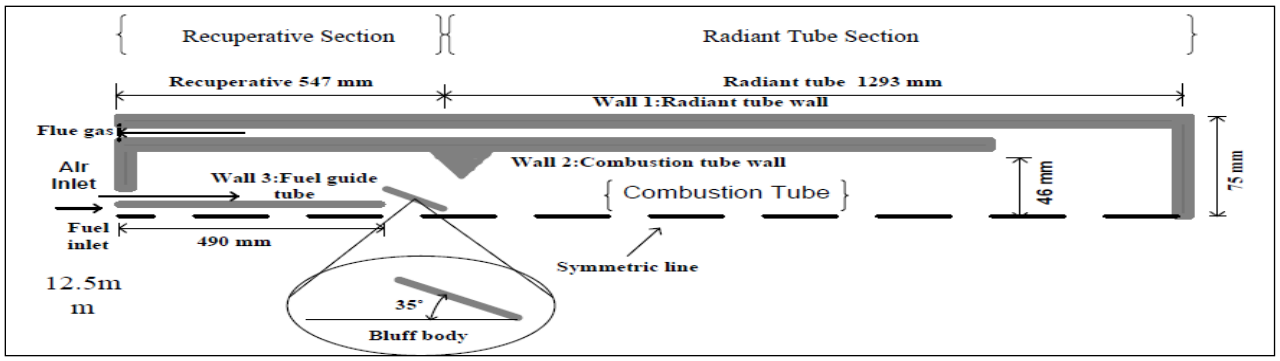

Figure 1. 2-D illustration of geometry of Case I, showing the grid dimensions, the boundaries and the dimensions of the domain.

3. Radiation models

3.1. Discrete Transfer Radiation Method (DTRM)

The equation for the change of radiant intensity, dI, along a path, ds, as given by Ilbas(2005) is as follows:

$$\frac{\mathbf{d}\boldsymbol{I}}{\mathbf{d}\boldsymbol{s}} + \boldsymbol{aI} = \frac{\boldsymbol{a\sigma T^4}}{\boldsymbol{\pi}} \qquad \textbf{(1)}$$

Where: a, $\boldsymbol{I}$, T and $\boldsymbol{\sigma}$ are gas absorption coefficient, intensity, gas local temperature and Stefan–Boltzmann constant (5.672×10^{-8} W/m^2 K^4) respectively. If a is constant along the ray, then $\boldsymbol{I}(\boldsymbol{s})$can be estimated as:

$$\boldsymbol{I(s)} = \frac{\boldsymbol{\sigma T^4}}{\boldsymbol{\pi}}(\mathbf{1} - \mathbf{exp}[-\boldsymbol{as}]) + \boldsymbol{I_0}\mathbf{exp}[-\boldsymbol{as}] \qquad \textbf{(2)}$$

Where, I_0 is the radiant intensity at the start of the incremental path, which is determined by the appropriate boundary condition. The energy source in the fluid due to radiation is then computed by summing the change in intensity along the path of each ray that is traced through the fluid control volume.

3.2. Weighted Sum of Gray Gas Model

The WSGGM is a reasonable compromise between the over-simplified gray gas model and a complete model which takes into account particular absorption bands. The basic assumption of the WSGGM is that the total emissivity over the distance s can be presented as written by Bidi et al (2008):

$$\boldsymbol{\varepsilon} = \sum_{\boldsymbol{i=0}}^{\mathbf{1}} \boldsymbol{a_{\varepsilon,i}(T)}[\mathbf{1} - \boldsymbol{e^{-k_i ps}}] \qquad \textbf{(3)}$$

Where $a_{\varepsilon,i}$is the emissivity weighting factors for the ith fictitious gray gas, the bracketed quantity is the ith fictitious gray gas emissivity, k_i is the absorption coefficient of the ith gray gas, p is the sum of the partial pressures of all absorbing gases, and s is the path length. The obtained values can be implemented for $a_{\varepsilon,i}$ and k_i R. Siegel (2002): and the values implemented in FLUENT are obtained from A. Coppalle(1983) and T. F. Smith (1982). These values depend on gas composition, and $a_{\varepsilon,i}$ also depends on the temperature.

4. CFD Set up

The numerical simulations are carried out using commercial CFD code FLUENT 6.2 using its built-in sub models and algorithms. Computational domains are created in GAMBIT. Axisymmetric grid domains containing 82,316 cells are generated for the SET burner. Mesh sensitivity study is conducted by increasing number of grids in the main fluid domains to ensure the current grid gave stable grid independent solutions with reasonable computational time.

Exploring the effect of combustion and radiation models in particular, to use the appropriate simulation to investigate the detailed fluid flow, combustion and heat transfer characteristics of the design.

Two radiation tubes with different fuel inputs at a heat duty of 31.56 kW, 18.39 kW with 5% of excess air is provided for the combustion. The chemical reactions in the methane combustion process in the SET burner are simulated using simple two-step reactions and the standard κ-ε turbulent model is applied in this research to simulate the turbulent flow inside the SET burner.

5. Results and Discussion

5.1. CFD Simulations of the Combustion Process Inside the SET Burners

Two standard cases are set up for the real fuel/air inlet conditions using the geometry shown in Fig. 1.In the standard cases (CFD case 1 and CFD case 2), which are evaluated with an experimental work carried out by Elmabrouk et al (2012), the boundary conditions are similar to real cases in the experimental measurement. The air inlet section area is 1.14×10^{-3} m^2 and the fuel inlet section area as 1.227×10^{-4} m^2. Boundary conditions of the CFD cases are shown in table 1.

Table 1. Boundary conditions of the axi-symmetric CFD simulations. All the Cases were carried out at excess air of 5% (equivalent ratio of 0.952)

CFD Cases	Boundary conditions					
	Fuel (Methane)		Air		Radiant Tube Surface Temperature (K)	CO_2 inlet velocity (m/s)
	Inlet Temperature (K)	Inlet Velocity (m/s)	Inlet Temperature (K)	Inlet Velocity (m/s)		
CFD case 1	300	6.93	300	8.91	1258	
CFD case 2	300	4.04	300	5.192	1248	
CFD case 3	300	6.93	300	8.91	1258	/
CFD case 4	300	6.93	300	8.91	1258	1.15 at 1380K
CFD case 5	300	6.93	300	8.91	1258	1.643 at 1380 K
CFD case 6	300	4.04	650	10.748	1248	/
CFD case 7	300	4.04	900	14.88	1248	/

5.2. The Effect of Bluff Body on the Combustion Process inside SET Burner

CFD Case 3 with the same boundary conditions of CFD Case 1 is carried out to investigate the influence of the bluff body inside the combustion chamber on the process of combustion, flame stabilisation and the efficiency of the burner, where bluff budy is not implemented in CFD Case 3.

Fig 2. and Fig 3. illustrate the turbulent rate of reaction for CFD Case 1 and CFD Case 3. In CFD Case 1, the reaction rate is much higher and more intense compared to CFD Case 3. In a

comparison with CFD Case 1, it is obvious from Fig 3. that the combustion reaction takes place far from the injection nozzle, and as stated by Peter Mullinger, P et al (2008), this consequence could limit the receiving feedback of heat from the reaction to maintain ignition on.

CFD case 1 and CFD case 3 demonstrate a difference in temperature distribution inside the burner, The temperature profile along the axial symmetry for these two cases is shown in Fig 4, where the temperature is much more uniforms for the CFD case 1 compared with CFD 3. The energy output (efficiency) is not different in these two cases, where the total heat transfers out from the radiant tube surface for each case is respectively 19.8 kW and 19.7 kW.

The peak temperature for CFD Case 1 is higher than the peak temperature for CFD Case 3; 2470 K and 2260 K respectively. The peak flame temperature for the first case is down in the middle of the combustion tube and is closer to the tube end for the second case. Consequently, the radiant tube in the second case can be directly exposed to the thermal stress and the bluff body would offer longer life service for the SET burner.

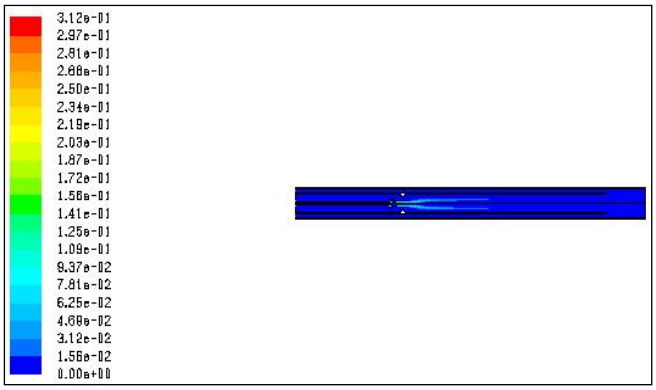

Figure 2. Contours of turbulent rate of reaction for CFD Case 1. (Kgmole/m^3-s).

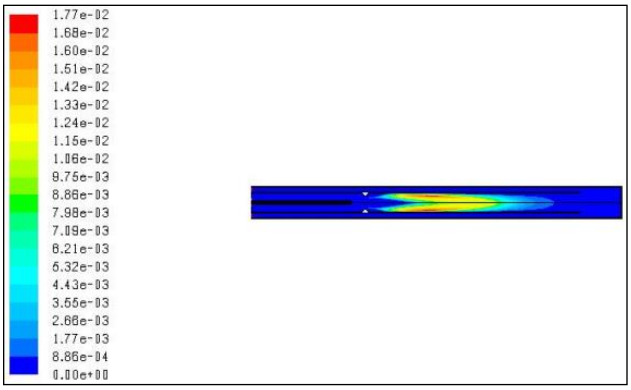

Figure 3. Contours of turbulent rate of reaction for CFD Case 3 (kgmol/m^3 –s)

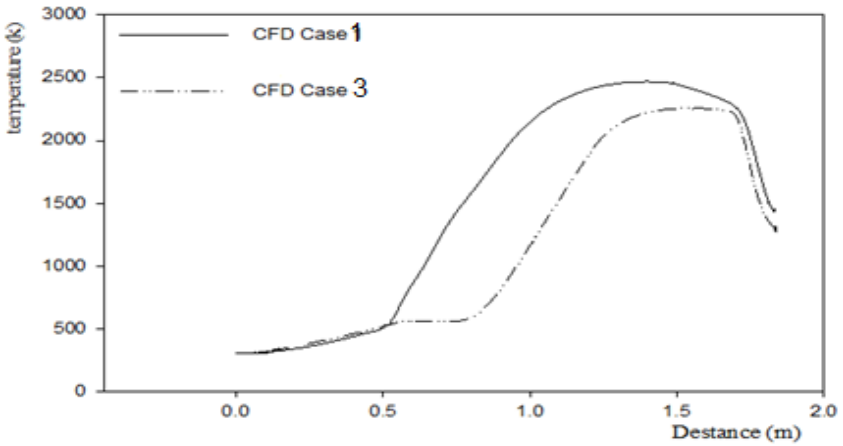

Figure 4. Temperature profile along the central line of the combustion tube

5.3. Effect of Flue Gas Recirculation

The process of flue gas recycling in a SET burner is tested to investigate its influence on the flame peak temperature and consequently on the SET burner thermal efficiency, by numerically introducing CO_2 at high temperature into the system at normal operational conditions. CO_2 is introduced at a temperature of 1380K, assuming that it is being internally recycled.

Flue gas recirculation increases the inert gases content of a mixture and therefore limits the combustion flammability of hydrocarbons and air. Flammable mixtures can be achieved with a recirculation rate of $K_V < 0.5$. As summarised by Wünning, J. A et al (1997) and Plessing, T et al (1998), in order to provide reliable operating conditions in practical systems, exhaust gas recirculation rates of $K_V < 0.3$ are used as a NO_x reduction technique. Two different calculations were carried out, based on the fact that 07% and 10% respectively of the required air is recycled in the combustion section. The recirculation rate is defined by Wünning, J. A. et al (1997) and Plessing, T et al (1998) as follows:

$$K_V = \frac{\dot{M}_E}{\dot{M}_F + \dot{M}_A} \qquad \textbf{(4)}$$

Both CFD Case 4 and CFD Case 5 are carried out with flue gas recirculation rates of K_V of 0.067 and 0.068 respectively. Fig 6 and Fig 7, show that the circulated flue gas reduces the flame peak temperature to 2300 K compared with CFD Case 1 illustrated in Fig 5, where the gas recirculation is not considered, and the flame peak temperature is 2470 K. However, by slightly increasing the exhaust gas recirculation rates to 0.068 (10% of the required air is introduced into the system) the reduction of flame peak temperature is limited as shown in Fig 7. It is therefore, possible to limit the thermal NO_x formation by the flue gas recycling technique in the SET burner application.

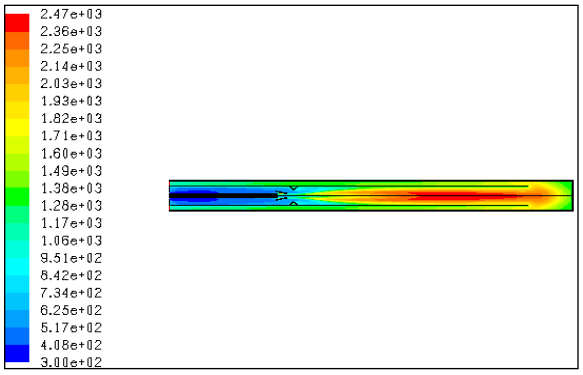

Figure 5. Contours of static temperature for CFD Case1 (K)

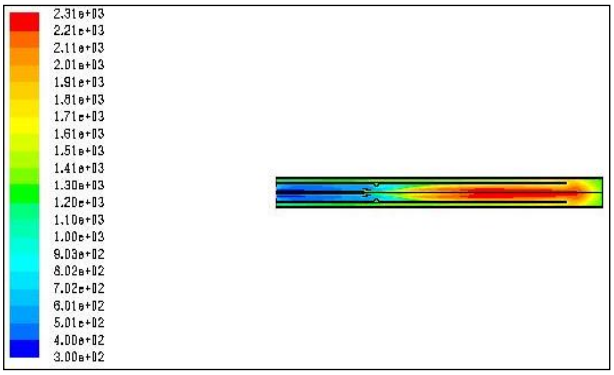

Figure 6. Contours of Static Temperature for **CFD Case 8 (flue** gas circulation K_V=0.067)

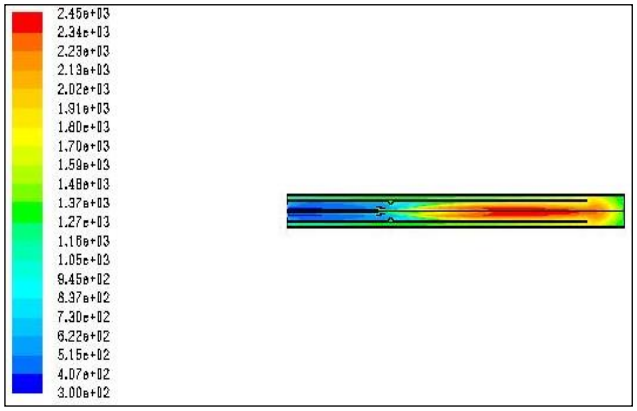

Figure 7. Contours of Static Temperature for CFD Case 9 (flue gas circulation K_V=0.068).

5.4. Effect of High Temperature Air Combustion (HiTAC)

Two different CFD cases are run to simulate the combustion and heat transfer processes inside the SET burner within HiTAC parameters. This is done to investigate the performance of the burners at these conditions, comparing them with CFD case 2. The first case is set at an air inlet temperature of 650 K and the second case set at an air inlet temperature of 900 K. The other boundary conditions for these two CFD cases are the same as the CFD Case 2 as indicated in table 1.

Fig 8 shows that the air inlet temperature reaches 1100K before the combustion zone, and e flame peak temperature is 2670K. Fig 11 shows that the HiTAC technique could provide better temperature distribution along the inner surface of the radiant tube burner compared with CFD Case 2. The HiTAC technique would improve the fuel saving and consequently, limit the environmental potential problems that may be caused by a higher flame peak temperature.

Fig 9 and Fig 10 show that the high concentration spot of CO species is far from the end of the radiant tube burner for CFD Case 6. As illustrated in Fig 8, the high flame temperature spot is far from the radiant tube end for CFD Case 6 and CFD Case 7 compared with CFD Case 1. And therefore, HiTAC technique could therefore provide better radiant tube burner life service.

The negative aspect of this technique is the increasing of thermal NO_x formation; and to overcome the trade-off between energy saving and the reduction of NO_x formation, Plessing, T et al (1998) suggested that flame cooling methods such as two-stage combustion and exhaust gas recirculation may be applied to lower the temperature within the combustion zone.

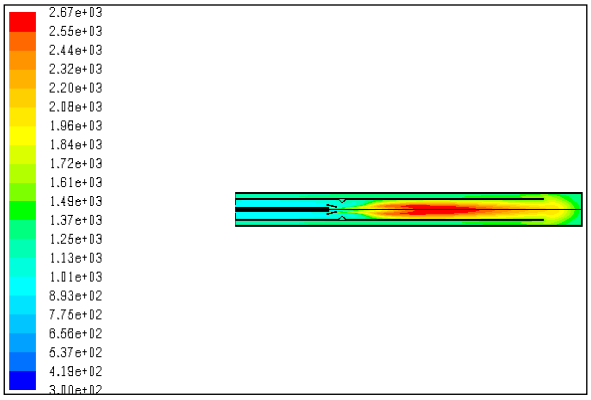

Figure 8. Contours of static temperature for CFD Case 11

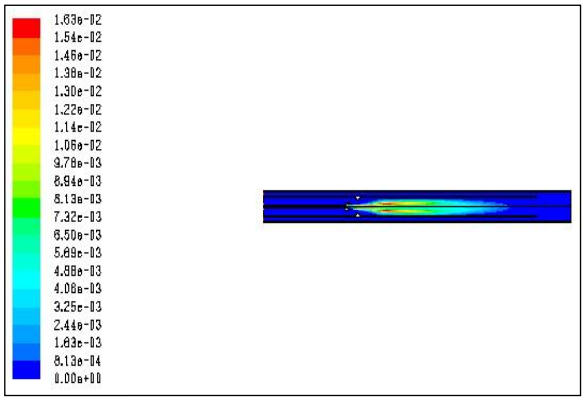

Figure 9. Contours of mass fraction of CO of CFD Case 1

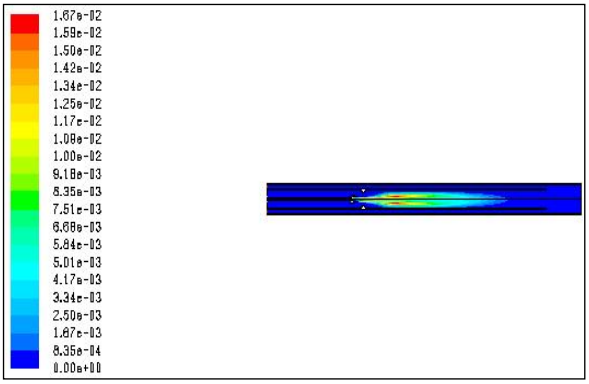

Figure 10. Contours of mass fraction of CO of CFD Case 11

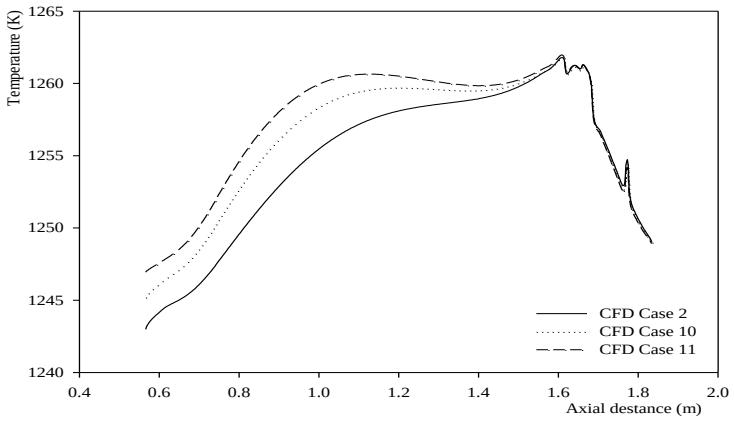

Figure 11. Temperature profile along the inner surface of the radiant tube

5.5. Heat fluxes and burner thermal efficiency.

The burner efficiency is evaluated based on thermal efficiency. In the other words based on radiation efficiency as a result of total heat transfer from the radiant tube to the surroundings. The radiation efficiency calculated as follows Galletti, C et al (2007):

$$\eta_{rad} = \frac{\dot{Q}}{\dot{Q}_{in}} \qquad \textbf{(5)}$$

Where, $\dot{Q}$ is the total heat transfer from the radiant tube to the surrounding atmosphere, and $\dot{Q}_{in}$ is the total input energy. Table 2. illustrates total input energy, the heat transfer rate to the surrounding and the burner efficiency for different cases. The main source of energy input is the heat released from combustion, while air inlet energy and fuel inlet energy are neglected. In the case of HiTAC, the air inlet energy was taken into account while calculating the energy input.

Flue gas recirculation has lowered the flame temperature, which is desirable for the reduction of NO_x formation, but it shows a very slightly improvement in burner efficiency. Flue gas circulation does not seem to have a major effect on the burner efficiency in terms of energy savings. A slight increase in burner efficiency was noted in CFD Case 4 and CFD Case 5, respectively 63% and 63.04% comparing with 62% the burner efficiency of CFD Case 1.

As shown in table 2, the SET burner is most efficient with HiTAC technology. The burner efficiency for CFD Case 6 is 87.7%, while the efficiency for CFD Case 7 is over 96%. These cases are compared with CFD Case 2 with 72% burner efficiency.

Table 2. Energy input, useful energy and burner efficiency

CFD Cases	$\dot{Q}_{in}$ (kW)	$\dot{Q}$ (kW)	η_{rad}
CFD Case 1	31.56	19.7	62%
CFD Case 2	18.4	13.2	72%
CFD Case 4	31.56	19.88	63%
CFD Case 5	31.56	19.89	63%
CFD Case 6	18.39 + 0.12	16.2	87%
CFD Case 7	18.39 + 0.227	18	96%

6. Conclusion

Based on the numerical investigation carried out in this research; it is found that the effect of the bluff body prevents the direct expose of the peak flame temperature to the radiant tube end, and consequently, leads to better operation conditions. Also, it is found that, flue gas circulation does not seem to have a major effect on the efficiency of the burner in terms of energy saving. This result appears to verify the simplification assumption of not simulating the flue gas recirculation. Flue gas circulation led to a decrease in the flame peak temperature and potentially reduced the NO_x formation process. Based on interesting results from 7 case studies it is evident that HiTAC

is numerically better to improve the radiant tube burner efficiency. Finally it is concluded that HiTAC highly improves the burner efficiency, but the high peak flame temperature does limit this application due to the environmental issues. Further flame cooling methods such as two-stage combustion and exhaust gas recirculation if applied does lower the temperature within the combustion zone.

References

[1] Bidi, M., Hosseini, R. and Nobari, M. R. H. (2008). "Numerical analysis of methane-air combustion considering radiation effect." Energy Conversion and Management**49**(12): 3634-3647.

[2] Coppalle, A. and Vervisch, p. (1983). "The Total Emissivities of High-Temperature Flames." Combustion and Flame**49**: 101-108.

[3] Elmabrouk. E. M and Wu. Y. (2012). "Enhancing the heat transfer in a heat treatment furnace through improving the combustion process in the radiation tubes" *IMA Journal of Applied Mathematics* (2012) 77, 59−71

[4] Hottel, H. C. and Sarofim, A. F. (1967). Radiative Transfer. New York, McGraw-Hill.

[5] Ilbas, M. (2005). "The effect of thermal radiation and radiation models on hydrogen-hydrocarbon combustion modelling." International Journal of Hydrogen Energy**30**(10): 1113-1126.

[6] Galletti, C., Parente, A. and Tognotti, L. (2007). "Numerical and experimental investigation of a mild combustion burner." Combustion and Flame **151**(4): 649-664.

[7] Guihua, H., Honggang, W. and Feng, Q. (2011). "Numerical simulation on flow, combustion and heat transfer of ethylene cracking furnaces." Chemical Engineering Science**66**(8): 1600-1611.

[8] Katsuki, M. and Hasegawa, T. (1998). The science and technology of combustion in highly preheated air. 27th Symposium (International) on Combustion. University of Colorado at Boulder**:** 3135-3146.

[9] Keramida, E. P., Liakos, H. H., Founti, M. A., Boudouvis, A. G. and Markatos, N. C. (2000). "Radiative heat transfer in natural gas-fired furnaces." International Journal of Heat and Mass Transfer**43**(10): 1801-1809.

[10] Masters, J., Webb, R. J. and Davies, R. M. (1979). "Use of Modelling Techniques in the Design and Application of Recuperative Burners." Journal of the Institute of Energy **52**(413): 196-204

[11] Plessing, T., Peters, N. and Wünning, J. G. (1998). "Laseroptical investigation of highly preheated combustion with strong exhaust gas recirculation." Symposium (International) on Combustion **27**(2): 3197-3204.

[12] Ramamurthy, H., Ramadhyani, S. and Viskanta, V. (1995). "*A Thermal System Model for a Radiant-Tube Continuous Reheating Furnace*." Journalof Materials Engineering and Performance**4**: 519-531.

[13] Siegel, R. and Howell, J., R (2002). Thermal radiation heat transfer. Washington, Hemisphere Publishing Corporation.

[14] Siegel, R. and Howell, J., R (1992). thermal radiation heat transfer, McGraw-Hill,.

[15] Smith, T., F, Shen, Z., F and Friedman, J., N (1982). "Evaluation of Coefficients for the Weighted Sum of Gray Gases Model." J. Heat Transfer**104**: 602-608.

[16] Wünning, J. A. and Wünning, J. G. (1997). "Flameless oxidation to reduce thermal no-formation." Progress in Energy and Combustion Science **23**(1): 81-94.

[17] Yu, M. J., Baek, S. W. and Park, J. H. (2000). "An extension of the weighted sum of gray gases non-gray gas radiation model to a two phase mixture of non-gray gas with particles." International Journal of Heat and Mass Transfer**43**(10): 1699-1713